Transient Analysis of Partitioned-Block Frequency-Domain Adaptive Filters

Feiran Yang[1], Gerald Enzner[2], Jun Yang[1]
1 Key Laboratory of Noise and Vibration Research, Institute of Acoustics, Chinese Academy of Sciences
2 Ruhr-Universität Bochum, Department of Electrical Engineering and Information Technology
Email: {feiran@mail.ioa.ac.cn; gerald.enzner@rub.de; jyang@mail.ioa.ac.cn}

***Abstract*—The frequency-domain adaptive filter (FDAF) is very useful for instance acoustic signal processing. The partitioned-block FDAF (PBFDAF) is a generalization of the FDAF and becomes more popular due to its low latency. Some efforts have been done toward the convergence analysis of PBFDAFs, but they usually use strong approximations and hence came to inaccurate results. This paper presents a unified approach to the transient analysis of both the constrained and unconstrained PBFDAFs based on the overlap-save structure. Using the independence assumption, we derive the analytical expressions for the mean and mean-square performance of PBFDAFs. Our analysis does not assume a specific model for the inputs and provides a quite general framework. Computer simulations confirm a good match between our theory and experimental results.**

***Index Terms*—Adaptive filtering, frequency domain, convergence analysis, transient behavior**

I. Introduction

In many applications, such as acoustic system identification [1]–[3], equalization [4], radar and communications [5], a long FIR filter is required. The time-domain adaptive filters are computationally inefficient for such an application [6]–[8]. An attractive solution to this problem is to adopt the frequency-domain adaptive filter (FDAF) [9]–[12], which achieves a significant computational saving using the FFT. However, the FDAF introduces two-block latency for data collecting and algorithm execution. Though the delayless structure can be employed to remove the delay [13]–[15], it is undesired to implement the FFT with large size. The partitioned block FDAF (PBFDAF) was then introduced to reduce the algorithm latency by splitting the impulse response into several smaller-size sub-filters [16]–[21].

Many efforts have been devoted toward the statistical convergence analysis of the FDAFs [22]–[29]. However, only a few studies focused on the analysis of the PBFDAF algorithm [30]–[34]. The relationship between the convergence properties and the number of partitions was investigated in [30]. The matrices that control the mean weight behavior of a family of PBFDAF algorithms were comprehensively analyzed based on the eigenvalue evaluation in [33]. The transient performance of the PBFDAF was presented in [31], [32] using strong approximations on the moment matrices, and hence the theoretical results are not accurate. In [34], a convergence analysis of the constrained PBFDAF was performed in the interest of concluding an optimal step size.

This paper presents an analytical model for the transient performance of a family of the PBFDAF algorithm with 50% overlap. The update equations of the constrained and unconstrained PBFDAFs are rewritten in a unified and compact form that is beneficially used for the convergence analysis. We derive the expressions for the mean-square deviation (MSD) and mean-square error (MSE) learning curves using the independence assumption and the 'vec' operation. Computer simulations are carried out to verify the theoretical predictions.

This work was supported by the Strategic Priority Research Program of Chinese Academy of Sciences under Grant XDC02020400, National Natural Science Fund of China under Grant 61501449, Youth Innovation Promotion Association of Chinese Academy of Sciences under Grant 2018027, and IACAS Young Elite Researcher Project QNYC201812.

II. PBFDAF Algorithms

We revisit the PBFDAF in a system identification problem. The desired signal $d(n)$ arises from the linear model

$$d(n) = \mathbf{x}^T(n)\mathbf{w} + v(n), \tag{1}$$

where $(\cdot)^T$ denote the transpose operation, $\mathbf{w} = [w_0, ..., w_{N-1}]^T$ is the weight vector of the unknown system of length N, $\mathbf{x}(n) = [x(n), ..., x(n-N+1)]^T$ is the input signal vector, and $v(n)$ denotes the independent system noise.

An adaptive filter $\hat{\mathbf{w}}(n)$ of length N is used to identify the unknown plant. In the PBFDAF algorithm [7], the model filter $\hat{\mathbf{w}}(n)$ is partitioned into P smaller-size segments as $\hat{\mathbf{w}}(n) = [\hat{\mathbf{w}}_0^T(n), ..., \hat{\mathbf{w}}_{P-1}^T(n)]^T$, where $\hat{\mathbf{w}}_p(n) = [\hat{w}_{pL}(n), ..., \hat{w}_{(p+1)L-1}(n)]^T$ is the p-th subfilter with $L = N/P$ taps. Thus, the error signal can be written as

$$e(n) = d(n) - \sum_{p=0}^{P-1} \bar{\mathbf{x}}_p^T(n)\hat{\mathbf{w}}_p(n), \tag{2}$$

where $\bar{\mathbf{x}}_p(n) = [x(n-pL), ..., x(n-(p+1)L+1)]^T$. Each of the linear convolutions in (2) can be computed efficiently using the FFT. The frequency-domain input matrix of the p-th partition is

$$\begin{aligned}\mathbf{X}_p(k) &= \mathrm{diag}\{[X_{p,0}(k), ..., X_{p,2L-1}(k)]^T\} \\ &= \mathrm{diag}\{\mathbf{F}\mathbf{x}_p(k)\},\end{aligned} \tag{3}$$

where k is the frame index, $\mathrm{diag}(\cdot)$ creates a diagonal matrix, $\mathbf{F}$ is the Fourier matrix of size $2L \times 2L$, and $\mathbf{x}_p(k) =$

978-9-0827-9703-9/19/$31.00 ©2019 IEEE

$[x((k-p-1)L),...,x((k-p+1)L-1)]^T$. The frequency-domain weight vector of the p-th partition is

$$\begin{aligned}\hat{\mathbf{W}}_p(k) &= \mathbf{F}[\hat{\mathbf{w}}_p^T(kL), \mathbf{0}_{1\times L}]^T \\ &= [\hat{W}_{p,0}(k),...,\hat{W}_{p,2L-1}(k)]^T.\end{aligned} \tag{4}$$

The frequency-domain error signal vector $\mathbf{E}(k)$ reads

$$\begin{aligned}\mathbf{E}(k) &= \mathbf{D}(k) - \mathbf{G}^{01}\sum_{p=0}^{P-1}\mathbf{X}_p(k)\hat{\mathbf{W}}_p(k) \\ &= [E_0(k),\cdots,E_{2L-1}(k)]^T,\end{aligned} \tag{5}$$

where $\mathbf{D}(k) = \mathbf{F}[\mathbf{0}_{1\times L}, d(kL),...,d(kL+L-1)]^T$ is the frequency-domain desired signal vector, and $\mathbf{G}^{01} = \mathbf{F}\begin{bmatrix}\mathbf{0}_L & \mathbf{0}_L \\ \mathbf{0}_L & \mathbf{I}_L\end{bmatrix}\mathbf{F}^{-1}$ is the windowing matrix that forces the first L elements to zero (the notations $\mathbf{0}_{1\times L}$, $\mathbf{0}_L$ and $\mathbf{I}_L$ being the $1\times L$ all-zero vector, $L\times L$ zero and identity matrices).

There are two kinds of PBFDAF algorithms, namely, the constrained version and unconstrained version. The update equation of the unconstrained PBFDAF is [7], [33]

$$\hat{\mathbf{W}}_p(k+1) = \hat{\mathbf{W}}_p(k) + \mu\mathbf{\Lambda}^{-1}\mathbf{X}_p^H(k)\mathbf{E}(k). \tag{6}$$

where $(\cdot)^H$ denote Hermitian operator, μ is the step size, and $\mathbf{\Lambda} = \mathcal{E}[\mathbf{X}_0^H(k)\mathbf{X}_0(k)]$ is the power spectral density matrix of the input signal ($\mathcal{E}[\cdot]$ being the mathematical expectation). In practice, the PSD matrix $\mathbf{\Lambda}$ can be estimated through recursively smoothing the DFT coefficients [7], [11].

The update equation of the constrained PBFDAF is [7], [16]

$$\hat{\mathbf{W}}_p(k+1) = \mathbf{F}\mathbf{Q}^{10}\mathbf{F}^{-1}[\hat{\mathbf{W}}_p(k) + \mu\mathbf{\Lambda}^{-1}(k)\mathbf{X}_p^H(k)\mathbf{E}(k)], \tag{7}$$

where $\mathbf{Q}^{10} = \begin{bmatrix}\mathbf{I}_L & \mathbf{0}_L \\ \mathbf{0}_L & \mathbf{0}_L\end{bmatrix}$ is the constraint matrix that constrains the last L time-domain elements of $\hat{\mathbf{W}}_p(k+1)$ to zero.

Using (6) and (7), we can write the update equations of the constrained and unconstrained PBFDAFs in a unified form

$$\hat{\mathbf{W}}_p(k+1) = \mathbf{G}^{10}[\hat{\mathbf{W}}_p(k) + \mu\mathbf{\Lambda}^{-1}\mathbf{X}_p^H(k)\mathbf{E}(k)], \tag{8}$$

where $\mathbf{G}^{10} = \mathbf{F}\mathbf{Q}^{10}\mathbf{F}^{-1}$ for the constrained version, and $\mathbf{G}^{10} = \mathbf{I}_{2L}$ for the unconstrained version.

We found that it is somewhat tedious to carry out the convergence analysis using (8). To alleviate the difficulty, we firstly define a super input matrix $\mathbf{X}(k)$ with size $2L\times 2LP$

$$\mathbf{X}(k) = [\mathbf{X}_0(k) \quad \mathbf{X}_1(k)\cdots\mathbf{X}_{P-1}(k)]. \tag{9}$$

We then construct a super weight vector $\hat{\mathbf{W}}(k)$ with size $2LP\times 1$ by stacking all the sub-weight vectors

$$\hat{\mathbf{W}}(k) = [\hat{\mathbf{W}}_0^T(k) \quad \hat{\mathbf{W}}_1^T(k)\cdots\hat{\mathbf{W}}_{P-1}^T(k)]^T. \tag{10}$$

Using (9) and (10), we can rewrite (5) in a matrix-vector formulation

$$\mathbf{E}(k) = \mathbf{D}(k) - \mathbf{G}^{01}\mathbf{X}(k)\hat{\mathbf{W}}(k). \tag{11}$$

The update equation (8) can be represented more compactly as

$$\hat{\mathbf{W}}(k+1) = \mathbf{\mathcal{G}}^{10}[\hat{\mathbf{W}}(k) + \mu\mathbf{\mathcal{L}}^{-1}\mathbf{X}^H(k)\mathbf{E}(k)], \tag{12}$$

where $\mathbf{\mathcal{L}}$ and $\mathbf{\mathcal{G}}$ are both block diagonal matrices given by

$$\mathbf{\mathcal{L}} = \mathrm{blkdiag}\{\mathbf{\Lambda},\ldots,\mathbf{\Lambda}\} \tag{13}$$

$$\mathbf{\mathcal{G}}^{10} = \mathrm{blkdiag}\{\mathbf{G}^{10},\ldots,\mathbf{G}^{10}\}. \tag{14}$$

We will use (11) and (12) to analyze the transient behaviors of the two versions of PBFDAF.

III. Transient Analysis

A. Model and assumptions

Analogously to (2), we rewrite (1) as

$$d(n) = \sum_{p=0}^{P-1}\bar{\mathbf{x}}_p^T(n)\mathbf{w}_p + v(n) \tag{15}$$

where $\mathbf{w}_p = [w_{pL},...,w_{(p+1)L-1}]^T$. We then get a frequency-domain representation of the model in (1)

$$\mathbf{D}(k) = \mathbf{G}^{01}\sum_{p=0}^{P-1}\mathbf{X}_p(k)\mathbf{W}_p + \mathbf{V}(k), \tag{16}$$

where $\mathbf{W}_p = \mathbf{F}[\mathbf{w}_p^T, \mathbf{0}_{1\times L}]^T$ is the DFT of $\mathbf{w}_p$, and

$$\begin{aligned}\mathbf{V}(k) &= \mathbf{F}[\mathbf{0}_{1\times L}, v(kL),...,v(kL+L-1)]^T \\ &= [V_0(k),...,V_{2L-1}(k)]^T\end{aligned} \tag{17}$$

is the frequency-domain noise vector. We define a $2LP\times 1$ super vector $\mathbf{W}$ by stacking all the sub-weights together

$$\mathbf{W} = [\mathbf{W}_0^T \quad \mathbf{W}_1^T\cdots\mathbf{W}_{P-1}^T]^T. \tag{18}$$

Using (18), we can also write the desired signal vector (16) in a more compact form

$$\mathbf{D}(k) = \mathbf{G}^{01}\mathbf{X}(k)\mathbf{W} + \mathbf{V}(k). \tag{19}$$

Substituting (19) into (11) yields

$$\mathbf{E}(k) = \mathbf{G}^{01}\mathbf{X}(k)\tilde{\mathbf{W}}(k) + \mathbf{V}(k), \tag{20}$$

where $\tilde{\mathbf{W}}(k) = \mathbf{W} - \hat{\mathbf{W}}(k)$ is the frequency-domain weight error vector.

To make the analysis tractable, we adopt two assumptions. A1). The sequences $\mathbf{X}_i(k)$ and $\mathbf{V}(k)$ are zero-mean and stationary random processes, and the noise vector $\mathbf{V}(k)$ is independent of any other signals. A2). The frequency-domain weight error vector $\tilde{\mathbf{W}}_i(k)$ and the input sequence $\mathbf{X}_j(k)$ are independent of each other. The second one is the well-known independence assumption [5]–[8] and has been widely used for the statistical analysis of adaptive filters.

B. Mean weight behavior

Subtracting the true weight vector $\mathbf{W}$ from both sides of (12) and using the fact that $\hat{\mathbf{W}}(k) = \mathbf{\mathcal{G}}^{10}\hat{\mathbf{W}}(k)$, we have

$$\tilde{\mathbf{W}}(k+1) = \mathbf{\mathcal{G}}^{10}[\tilde{\mathbf{W}}(k) - \mu\mathbf{\mathcal{L}}^{-1}\mathbf{X}^H(k)\mathbf{E}(k)]. \tag{21}$$

Substituting (20) into (21), we get

$$\begin{aligned}\tilde{\mathbf{W}}(k+1) = \mathbf{\mathcal{G}}^{10}[&\tilde{\mathbf{W}}(k) - \mu\mathbf{\mathcal{L}}^{-1}\mathbf{X}^H(k)\mathbf{G}^{01}\mathbf{X}(k)\tilde{\mathbf{W}}(k) \\ &- \mu\mathbf{\mathcal{L}}^{-1}\mathbf{X}^H(k)\mathbf{V}(k)].\end{aligned} \tag{22}$$

Taking the mathematical expectation on both sides of (22) and using the above two assumptions, we obtain

$$\mathcal{E}[\tilde{\mathbf{W}}(k+1)] = \mathbf{S}\mathcal{E}[\tilde{\mathbf{W}}(k)], \tag{23}$$

where

$$\mathbf{S} = \boldsymbol{\mathcal{G}}^{10}\left\{\mathbf{I}_{2L} - \mu\mathcal{E}[\boldsymbol{\mathcal{A}}^H(k)]\right\}, \tag{24}$$

$$\boldsymbol{\mathcal{A}}(k) = \mathbf{X}^H(k)\mathbf{G}^{01}\mathbf{X}(k)\boldsymbol{\mathcal{L}}^{-1}. \tag{25}$$

The eigenvalue spread of the matrix $\mathbf{S}$ controls the mean convergence of the PBFDAF algorithm. A thorough analysis of the properties of $\mathcal{E}[\boldsymbol{\mathcal{A}}(k)]$ can be found in [33].

C. Mean-square convergence

Using (25), we can then rewrite (22) as

$$\begin{aligned}\tilde{\mathbf{W}}(k+1) = \boldsymbol{\mathcal{G}}^{10}[&\tilde{\mathbf{W}}(k) - \mu\boldsymbol{\mathcal{A}}^H(k)\tilde{\mathbf{W}}(k) \\ &- \mu\boldsymbol{\mathcal{L}}^{-1}\mathbf{X}^H(k)\mathbf{V}(k)].\end{aligned} \tag{26}$$

Multiplying both sides of (26) from the right by their respective Hermitian transposes and using the two assumptions, one has

$$\begin{aligned}&\mathcal{E}[\tilde{\mathbf{W}}(k+1)\tilde{\mathbf{W}}^H(k+1)] \\ &= \boldsymbol{\mathcal{G}}^{10}\big\{\mathcal{E}[\tilde{\mathbf{W}}(k)\tilde{\mathbf{W}}^H(k)] \\ &\quad - \mu\mathcal{E}[\tilde{\mathbf{W}}(k)\tilde{\mathbf{W}}^H(k)]\mathcal{E}[\boldsymbol{\mathcal{A}}(k)] \\ &\quad - \mu\mathcal{E}[\boldsymbol{\mathcal{A}}^H(k)]\mathcal{E}[\tilde{\mathbf{W}}(k)\tilde{\mathbf{W}}^H(k)] \\ &\quad + \mu^2\mathcal{E}[\boldsymbol{\mathcal{A}}^H(k)\tilde{\mathbf{W}}(k)\tilde{\mathbf{W}}^H(k)\boldsymbol{\mathcal{A}}(k)] \\ &\quad + \mu^2\mathcal{E}[\boldsymbol{\mathcal{L}}^{-1}\mathbf{X}^H(k)\boldsymbol{\Phi}_v\mathbf{X}(k)\boldsymbol{\mathcal{L}}^{-1}]\big\}\boldsymbol{\mathcal{G}}^{10},\end{aligned} \tag{27}$$

where $\boldsymbol{\Phi}_v = \mathcal{E}[\mathbf{V}(k)\mathbf{V}^H(k)]$ is the noise covariance matrix.

To obtain an analytical model for the mean square behaviors, we resort to the 'vec' operator that transforms the matrix into a vector [6]. To proceed, we first introduce a property of the 'vec' operator. For the matrices $\mathbf{M}$, $\mathbf{N}$ and $\boldsymbol{\Sigma}$ with compatible dimensions, the following relation holds [35]

$$\mathrm{vec}(\mathbf{M}\boldsymbol{\Sigma}\mathbf{N}) = (\mathbf{N}^T \otimes \mathbf{M})\mathrm{vec}(\boldsymbol{\Sigma}), \tag{28}$$

where $\mathrm{vec}(\cdot)$ creates a column vector through stacking the successive columns of the augmented matrix, and $\otimes$ stands for the Kronecker product.

Define a $(2LP)^2 \times 1$ vector $\mathbf{z}(k)$ that is constructed by stacking all the column vectors of the weight error covariance matrix $\mathcal{E}[\tilde{\mathbf{W}}(k)\tilde{\mathbf{W}}^H(k)]$

$$\begin{aligned}\mathbf{z}(k) &= \mathrm{vec}\left\{\mathcal{E}[\tilde{\mathbf{W}}(k)\tilde{\mathbf{W}}^H(k)]\right\} \\ &= \Big\{\mathcal{E}[\tilde{W}_{0,0}(k)\tilde{W}^*_{0,0}(k)], \mathcal{E}[\tilde{W}_{0,1}(k)\tilde{W}^*_{0,0}(k)], \\ &\quad \cdots, \mathcal{E}[\tilde{W}_{P-1,2L-1}(k)\tilde{W}^*_{P-1,2L-1}(k)]\Big\}^T \\ &\triangleq [z_{0,0,0,0}(k), z_{0,1,0,0}(k), \cdots, \\ &\quad z_{P-1,2L-1,P-1,2L-1}(k)]^T,\end{aligned} \tag{29}$$

such that $z_{p,i,q,j}(k) = \mathcal{E}[\tilde{W}_{p,i}(k)\tilde{W}^*_{q,j}(k)]$. Applying the 'vec' operator to both sides of (27) and using the property in (28), we then obtain a $(2LP)^2$-dimensional state recursion that describes the evolution of the mean-square learning curves of the PBFDAF algorithms

$$\mathbf{z}(k+1) = \boldsymbol{\Theta}\mathbf{z}(k) + \boldsymbol{\Psi}, \tag{30}$$

where

$$\boldsymbol{\Theta} = \left[(\boldsymbol{\mathcal{G}}^{10})^T \otimes \boldsymbol{\mathcal{G}}^{10}\right]\left(\mathbf{I}_{(2LP)^2} - \mu\mathbf{C} + \mu^2\mathbf{J}\right), \tag{31}$$

$$\boldsymbol{\Psi} = \mu^2[(\boldsymbol{\mathcal{G}}^{10})^T \otimes \boldsymbol{\mathcal{G}}^{10}]\mathrm{vec}\left\{\mathcal{E}[\boldsymbol{\mathcal{L}}^{-1}\mathbf{X}^H(k)\boldsymbol{\Phi}_v\mathbf{X}(k)\boldsymbol{\mathcal{L}}^{-1}]\right\} \tag{32}$$

with the $(2LP)^2 \times (2LP)^2$ matrices $\mathbf{C}$ and $\mathbf{J}$ given by

$$\mathbf{C} = \mathcal{E}[\boldsymbol{\mathcal{A}}^T(k)] \otimes \mathbf{I}_{2LP} + \mathbf{I}_{2LP} \otimes \mathcal{E}[\boldsymbol{\mathcal{A}}^H(k)], \tag{33}$$

$$\mathbf{J} = \mathcal{E}[\boldsymbol{\mathcal{A}}^T(k) \otimes \boldsymbol{\mathcal{A}}^H(k)]. \tag{34}$$

As indicated by (30), the eigenvalues of the matrix $\boldsymbol{\Theta}$ fully characterize the second-order convergence rate of various forms of the PBFDAF. It is interesting to study eigenvalue spread of $\boldsymbol{\Theta}$ for a better understanding of the mean-square behavior of various PBFDAFs, which is beyond the scope of this paper. The MSD learning curve of the PBFDAFs can then be computed by

$$\Delta(k) = \mathcal{E}\left(\left\|\tilde{\mathbf{W}}(k)\right\|^2\right) = \sum_{p=0}^{P-1}\sum_{i=0}^{2L-1} z_{p,i,p,i}(k). \tag{35}$$

We then evaluate the MSE learning curve of the PBFDAFs. Because the PBFDAF is implemented on a block-by-block basis, the MSE of the PBFDAF algorithm is given by [6]

$$\xi(k) = \frac{1}{L}\mathcal{E}\Big[\sum_{i=0}^{L-1} e^2(kL+i)\Big]. \tag{36}$$

Using the DFT properties, it is easy to show that $\xi(k)$ can be evaluated in the frequency domain directly

$$\xi(k) = \frac{1}{2L^2}\mathcal{E}[\mathbf{E}^H(k)\mathbf{E}(k)]. \tag{37}$$

Substituting (20) into (37) and using the two assumptions, we then obtain

$$\xi(k) = \xi_{\mathrm{ex}}(k) + \xi_{\min}, \tag{38}$$

where

$$\xi_{\min} = \frac{1}{2L^2}\mathcal{E}[\mathbf{V}^H(k)\mathbf{V}(k)] = \mathcal{E}[v^2(n)] \tag{39}$$

is the minimum MSE, and

$$\begin{aligned}\xi_{\mathrm{ex}}(k) &= \frac{1}{2L^2}\mathcal{E}[\tilde{\mathbf{W}}^H(k)\mathbf{X}^H(k)\mathbf{G}^{01}\mathbf{X}(k)\tilde{\mathbf{W}}(k)] \\ &= \frac{1}{2L^2}\mathrm{tr}\left\{\mathrm{vec}^{-1}[\mathbf{z}(k)]\mathcal{E}[\boldsymbol{\mathcal{B}}(k)]\right\}\end{aligned} \tag{40}$$

is the excess MSE (EMSE) introduced by perturbation of the estimated weight vector with $\boldsymbol{\mathcal{B}}(k) = \mathbf{X}^H(k)\mathbf{G}^{01}\mathbf{X}(k)$. Once the moment matrices are determined, the MSD and MSE learning curves of PBFDAFs can be accurately described by (30), (35) and (40).

The advantages of our theoretical analysis lie in three aspects. First, we do not assume the specific statistics of the input signals, i.e., the proposed theoretical model does not restrict the input data to being Gaussian or white. The required moment matrices can be evaluated under the knowledge of the input statistics in closed form [36], [37] or by the numerical method [6]. Second, we do not use any approximations on the moment matrices. Third, the correlations between different sub-filters are considered. The latter two aspects make our analysis model more accurate than the previous ones.

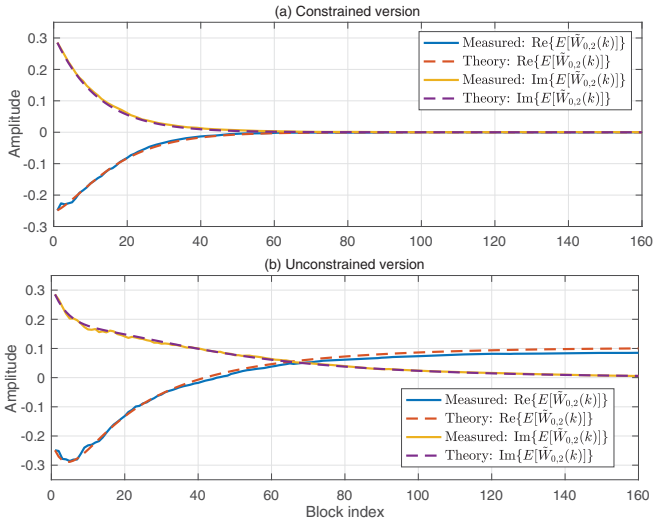

Fig. 1. Mean weight error vector behavior of $\mathcal{E}[\tilde{W}_{0,2}(k)]$. (a) Constrained PBFDAF. (b) Unconstrained PBFDAF.

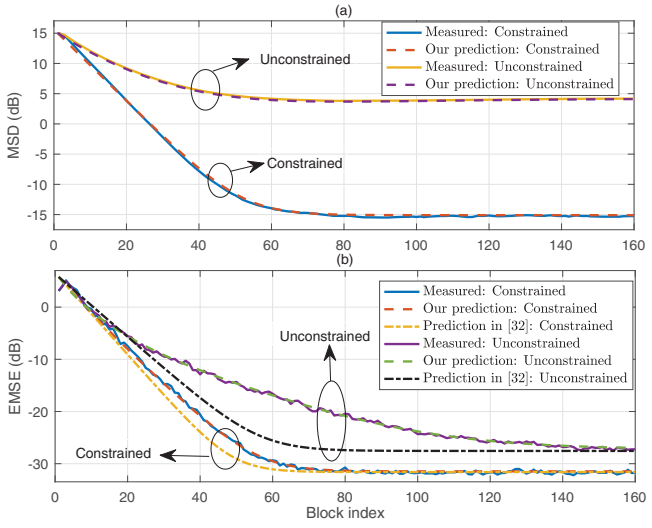

Fig. 2. Transient behaviors of constrained and unconstrained PBFDAFs. (a) MSD. (b) EMSE.

IV. Simulation Results

Computer simulations are carried out to verify the theoretical results. The lengths of the adaptive filter and each subfilter are $N = 48$ and $L = 16$, respectively. The coefficients of the unknown system is generated by a zero-mean white noise sequence with $\|\mathbf{w}\| = 1$. The input signal is an AR(1) process that is generated by filtering the uniformly distributed signal through the transfer function $H(z) = 1/(1 - 0.9z^{-1})$. White Gaussian noise is added to the desired signal. The signal-to-noise ratio (SNR) is 30 dB, and the step size is $\mu = 0.2$. The moment matrices are estimated via ensemble averaging. The adaptive weight vectors $\hat{\mathbf{W}}_p(0)$ are initialized as a zero vector. The experimental results are averaged over 100 independent trials.

Fig. 1 investigates the mean weight-error behavior of the PBFDAFs, where Fig. 1(a) and Fig. 1(b) correspond to the constrained and unconstrained versions, respectively. For presentation clarity, we only show the behaviors of the real and imaginary parts of the third coefficient of the first subfilter $\mathcal{E}[\tilde{W}_{0,2}(k)]$. The theoretical predictions are in good agreement with the experiment results. We found that the mean weight vector of the constrained PBFDAF can converge to the true solution, while that of the unconstrained version cannot. For the unconstrained PBFDAF, the special overlap structure of $\mathbf{x}_p(k)$ leads to the rank loss of the matrix $\mathcal{E}[\boldsymbol{\mathcal{A}}(k)]$, and hence the steady-state mean weight vector cannot converge to the optimal solution. That is, the bias is introduced by the control matrix $\mathcal{E}[\boldsymbol{\mathcal{A}}(k)]$ but not the initialization of the weight vector. It was stated in [33] that the mean weight behavior of the unconstrained PBFDAF 'appears as a kind of random walk stochastic process.' However, both the presented theory and experiment clearly indicate the mean weight curve of the unconstrained PBFDAF is deterministic but not stochastic once the initialized values are determined.

Fig. 2 depicts the analytical and experimental results for the mean-square performance of PBFDAFs. Our predicted MSD and EMSE learning curves are calculated using (35) and (40), respectively. The theoretical results in [32] are also involved for the performance comparison. It can be seen that our theoretical results coincide very closely with the experimental ones, while the theoretical curves from [32] considerably deviate from the experimental results especially during the transient phase. It is also observed that the steady-state MSD of the unconstrained PBFDAF is much higher than that of the constrained version, which is mainly because the mean weight vector of the unconstrained PBFDAF with 50% overlap cannot converge to the true solution. This indicates that the unconstrained PBFDAF is not suitable for the system identification application in which the exact system impulse response is required.

V. Conclusions

This paper presented an accurate transient analysis of a family of the overlap-save PBFDAF, including the mean weight error and the mean-square convergence behaviors. We did not assume the specific probability density function of the input signal. The proposed analytical models are well consistent with the experiment results. This paper revealed some new properties of PBFDAFs with 50% overlap, e.g., the mean weight vector of the constrained PBFDAF converges to the true solution, while that of the unconstrained version converges to a biased solution, leading to a larger misalignment. This is quite different from the FDAF algorithms, which converge to the optimal solution for both the constrained and unconstrained versions. The theoretical results could also be utilized to derive the step-size bound for the mean and mean-square stability, which is left as our future work.

REFERENCES

[1] E. Hänsler and G. Schmidt, *Acoustic Echo and Noise Control: A Practical Approach*. Wiley, 2004.

[2] P. Vary and R. Martin, *Digital Speech Transmission. Enhancement, Coding and Error Concealment*. Chichester, U.K.: Wiley, 2006.

[3] G. Enzner, H. Buchner, A. Favrot, and F. Kuech, "Acoustic echo control," in *Academic press library in signal processing*. Academic Press, 2014, pp. 807–877.

[4] P. A. Naylor and N. D. Gaubitch, *Speech Dereverberation*. Springer, 2010.

[5] S. Haykin, *Adaptive Filter Theory*. Prentice Hall, 2013.

[6] A. H. Sayed, *Fundamentals of Adaptive Filtering*. New York, NY, USA: Wiley-Inter-Science, 2003.

[7] B. Farhang-Boroujeny, *Adaptive Filters: Theory and Applications*. John Wiley & Sons, 2013.

[8] P. S. R. Diniz, *Adaptive Filtering: Algorithms and Practical Implementations*. Springer, Boston, MA, 2008.

[9] E. R. Ferrara, "Fast implementation of LMS adaptive filters," *IEEE Trans. Acoust., Speech, Signal Process.*, vol. 28, no. 4, pp. 474–475, Aug. 1980.

[10] G. A. Clark, S. R. Parker, and S. K. Mitra, "A unified approach to time and frequency domain realization of FIR adaptive digital filters," *IEEE Trans. Acoustic, Speech, Signal Process.*, vol. 31, no. 5, pp. 1073–1083, Oct. 1983.

[11] D. Mansour and A. H. Gray, Jr., "Unconstrained frequency-domain adaptive filter," *IEEE Trans. Acoust., Speech, Signal Process.*, vol. 30, no. 5, pp. 726–734, Oct. 1982.

[12] J. J. Shynk, "Frequency-domain and multirate adaptive filtering," *IEEE Signal Process. Mag.*, vol. 9, no. 1, pp. 14–37, Jan. 1992.

[13] D. R. Morgan and J. C. Thi, "A delayless subband adaptive filter architecture," *IEEE Trans. Signal Process.*, vol. 43, no. 8, pp. 1819–1830, Aug. 1995.

[14] R. Merched, P. S. R. Diniz, and M. R. Petraglia, "A new delayless subband adaptive filter structure," *IEEE Trans. Signal Process.*, vol. 47, no. 6, pp. 1580–1591, Jun. 1999.

[15] F. Yang, M. Wu, and J. Yang, "A computationally efficient delayless frequency-domain adaptive filter algorithm," *IEEE Trans. Circuits Syst. II*, vol. 60, no. 4, pp. 222–226, Apr. 2013.

[16] J. S. Soo and K. K. Pang, "Multidelay block frequency-domain adaptive filter," *IEEE Trans. Acoust., Speech, Signal Process.*, vol. 38, no. 2, pp. 373–376, Feb. 1990.

[17] P. C. W. Sommen, "Adaptive filtering methods," Ph.D. dissertation, Eindhoven University of Technology, 1992.

[18] G. Enzner and P. Vary, "A soft-partitioned frequency-domain adaptive filter for acoustic echo cancellation," in *Proc. IEEE ICASSP*, Oct. 2003, pp. 393–396.

[19] A. Spriet, G. Rombouts, M. Moonen, and J. Wouters, "Adaptive feedback cancellation in hearing aids," *J. Franklin Inst.*, vol. 343, no. 6, pp. 545–573, Sep. 2006.

[20] J. Lorente, M. Ferrer, M. D. Diego, and A. González, "GPU implementation of multichannel adaptive algorithms for local active noise control," *IEEE Trans. Audio, Speech, Lang. Process.*, vol. 22, no. 11, pp. 1624–1635, Nov. 2014.

[21] C. Hofmann, C. Huemmer, M. Guenther, and W. Kellermann, "Significance-aware filtering for nonlinear acoustic echo cancellation," *EURASIP Journal on Advances in Signal Processing*, vol. 2016, Nov. 2016.

[22] J. C. Lee and C. K. Un, "Performance analysis of frequency domain block LMS adaptive digital filters," *IEEE Trans. Circuits Syst.*, vol. 36, no. 2, pp. 173–189, Feb. 1989.

[23] P. C. W. Sommen, P. J. V. Gerwen, H. J. Kotmans, and A. J. E. M. Janssen, "Convergence analysis of a frequency domain adaptive filter with exponential power averaging and generalized window function," *IEEE Trans. Circuits Syst.*, vol. 34, no. 7, pp. 788–798, Jul. 1987.

[24] J. C. Lee and C. K. Un, "Performance analysis of frequency domain block LMS adaptive digital filters," *IEEE Trans. Circuits Syst.*, vol. 36, no. 2, pp. 173–189, Feb. 1989.

[25] A. Feuer and R. Cristi, "On the steady state performance of frequency domain LMS algorithms," *IEEE Trans. Signal Process.*, vol. 41, no. 1, pp. 419–423, Jan. 1993.

[26] B. Farhang-Boroujeny and K. S. Chan, "Analysis of the frequency-domain block LMS algorithm," *IEEE Trans. Signal Process.*, vol. 48, pp. 2332–2342, Aug. 2000.

[27] M. Wu, J. Yang, Y. Xu, and X. Qiu, "Steady-state solution of the deficient length constrained FBLMS algorithm," *IEEE Trans. Signal Process.*, vol. 60, no. 12, pp. 6681–6687, Dec. 2012.

[28] F. Yang, G. Enzner, and J. Yang, "Statistical convergence analysis for optimal control of DFT-domain adaptive echo canceler," *IEEE/ACM Trans. Audio, Speech, Lang. Process.*, vol. 25, pp. 1095–1106, May 2017.

[29] F. Yang, G. Enzner, and J. Yang, "A unified approach to the statistical convergence analysis of frequency-domain adaptive filters," *IEEE Trans. Signal Process.*, vol. 67, no. 7, pp. 1785–1796, Apr. 2019.

[30] P. C. W. Sommen, "On the convergence properties of a partitioned block frequency domain adaptive filter (PBFDAF)," in *Proc. EUSIPCO*, 1990, pp. 201–203.

[31] E. Moulines, O. A. Amrane, and Y. Grenier, "The generalized multidelay adaptive filter: Structure and convergence analysis," *IEEE Trans. Signal Process.*, vol. 43, no. 1, pp. 14–28, Jan. 1995.

[32] P. G. Estermann, A. Kaelin, and A. G. Lindgren, "Analysis of partitioned frequency-domain LMS adaptive algorithm with application to a hands-free telephone system echo canceller," *Int. J. Adapt. Contr. Signal Process.*, vol. 14, no. 6, pp. 587–608, Aug 2000.

[33] K. S. Chan and B. Farhang-Boroujeny, "Analysis of the partitioned frequency-domain block LMS (PFBLMS) algorithm," *IEEE Trans. Signal Process.*, vol. 49, no. 9, pp. 1860–1874, Sep. 2001.

[34] B. H. Nitsch, "A frequency-selective stepfactor control for an adaptive filter algorithm working in the frequency domain," *Signal Process.*, vol. 80, pp. 1733–1745, Sep. 2000.

[35] T. K. Moon and W. C. Stirling, *Mathematical Methods and Algorithms for Signal Processing*. New York, NY, USA: Prentice-Hall, 2000.

[36] T. Y. Al-Naffouri and M. Moinuddin, "Exact performance analysis of the ϵ-NLMS algorithm for colored circular Gaussian inputs," *IEEE Trans. Signal Process.*, vol. 58, no. 10, pp. 5080–5090, Oct. 2010.

[37] T. Y. Al-Naffouri, M. Moinuddin, and M. S. Sohail, "Mean weight behavior of the NLMS algorithm for correlated Gaussian inputs," *IEEE Signal Process. Lett.*, vol. 18, no. 1, pp. 7–10, Jan. 2011.